A compact low energy proton source

A. Weiser ✉ iD ; A. Lanz iD ; E. D. Hunter iD ; M. C. Simon iD ; E. Widmann iD ; D. J. Murtagh ✉ iD
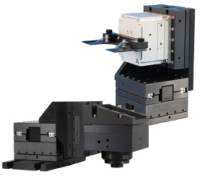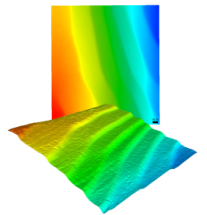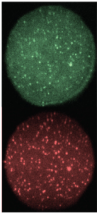
Check for updates

CrossMark

View Online

Export Citation

A compact low energy proton source

View Online   Export Citation   CrossMark

A. Weiser,[1,2,a] [ID]   A. Lanz,[1,2] [ID]   E. D. Hunter,[1] [ID]   M. C. Simon,[1] [ID]   E. Widmann,[1] [ID]   and D. J. Murtagh[1,a] [ID]

AFFILIATIONS

[1] Stefan-Meyer-Institute for Subatomic Physics, Austrian Academy of Sciences, Kegelgasse 27, 1030 Wien, Austria
[2] Vienna Doctoral School in Physics, University of Vienna, Vienna, Austria

[a]**Authors to whom correspondence should be addressed:** alina.weiser@oeaw.ac.at and daniel.murtagh@oeaw.ac.at

ABSTRACT

A low energy proton source for non-neutral plasma experiments was developed. Electrons from a hot filament ionize H_2 gas inside a geometrically compensated Penning trap to produce protons via dissociative ionization. A rotating wall electric field destabilizes the unwanted H_2^+ and H_3^+ generated in the process while concentrating protons at the center of the trap. The source produces bunches of protons with relatively low ion contamination (5.5% H_2^+ and 15.5% H_3^+), with energy tunable from 35 to 300 eV.

I. INTRODUCTION

The Atomic Spectroscopy And Collisions Using Slow Antiprotons (ASACUSA) Cusp experiment aims to measure the hyperfine splitting of antihydrogen in a magnetic field-free region.[1–4] The Cusp experiment produces antihydrogen via the three-body recombination process, i.e., $e^+ + e^+ + \bar{p} \rightarrow e^+ + \bar{H}$ in a nested Penning trap.[5] To produce a beam of atoms with the desired attributes (ground state, spin polarized, mean speed $v < 1000$ m/s), the plasma properties of the antiprotons and positrons must be optimized.

Optimizing the mixing process is challenging and requires repeated experiments with positron and antiproton plasmas. Positrons are produced by a ^{22}Na source and hence are available at any time. Trappable antiprotons are only available from CERN's Antiproton Decelerator (AD), which is not always online. For example, the entire complex was shut down for two years (2019–2021) while the LHC was upgraded. A low energy proton source allows ASACUSA to continue studying the mixing process during such periods by combining protons and electron plasma instead of antiprotons and positron plasma.

Such a source should preferably produce proton bunches comparable to those of the antiprotons as they enter the mixing trap ($\sim 10^5$ $\bar{p}$ every 110 s, $E_{kin} = 100$ eV), have a high proton fraction, and a good vacuum rating of $<10^{-6}$ mbar so that the beamlines and traps are not contaminated by the operation of the source.

Proton sources using different methods of ion production have been developed for various applications. Radio frequency sources such as electron cyclotron resonance (ECR) proton sources are commonly used in accelerator physics as they can create high energy

($\sim$10 keV), high current ($\sim$10 mA) proton beams with little H_2^+ and H_3^+ contamination.[6,7] Laser-driven proton sources can produce multi-MeV, ultra-short ($\sim$ps) proton bunches and have applications in, for example, proton radiography and material research.[8,9] The use of such complex apparatus is not necessary as such high currents and energies are not required for the planned operation. Instead, a much simpler and more compact device using just electron bombardment of a H_2 gas is sufficient. Small ion sources have been developed for other particle traps[10] and are also commercially available (e.g., SPECS, IQE 11/35) but they have not addressed the issue of active suppression of H_2^+ and H_3^+. The proton source discussed here uses electron impact ionization of H_2 gas and a Penning trap gas cell to produce a pulsed proton beam. In our case, H_2^+, and H_3^+ contaminants were reduced by applying a rotating wall (RW) electric field[11] using the azimuthally segmented central electrode of the gas cell. The proton source design and method of operation will be described in detail in Sec. II. Results from characterization measurements will be shown in Sec. III.

II. PROTON SOURCE

A schematic diagram of the low energy proton source is shown in Fig. 1(a). The source is constructed of three modules: A. electron gun, B. gas cell trap, and C. ion extraction and steering.

A. Electron gun

The electron beam is formed using a tungsten filament from Kimball Physics (ES-020), biased to the same potential as the
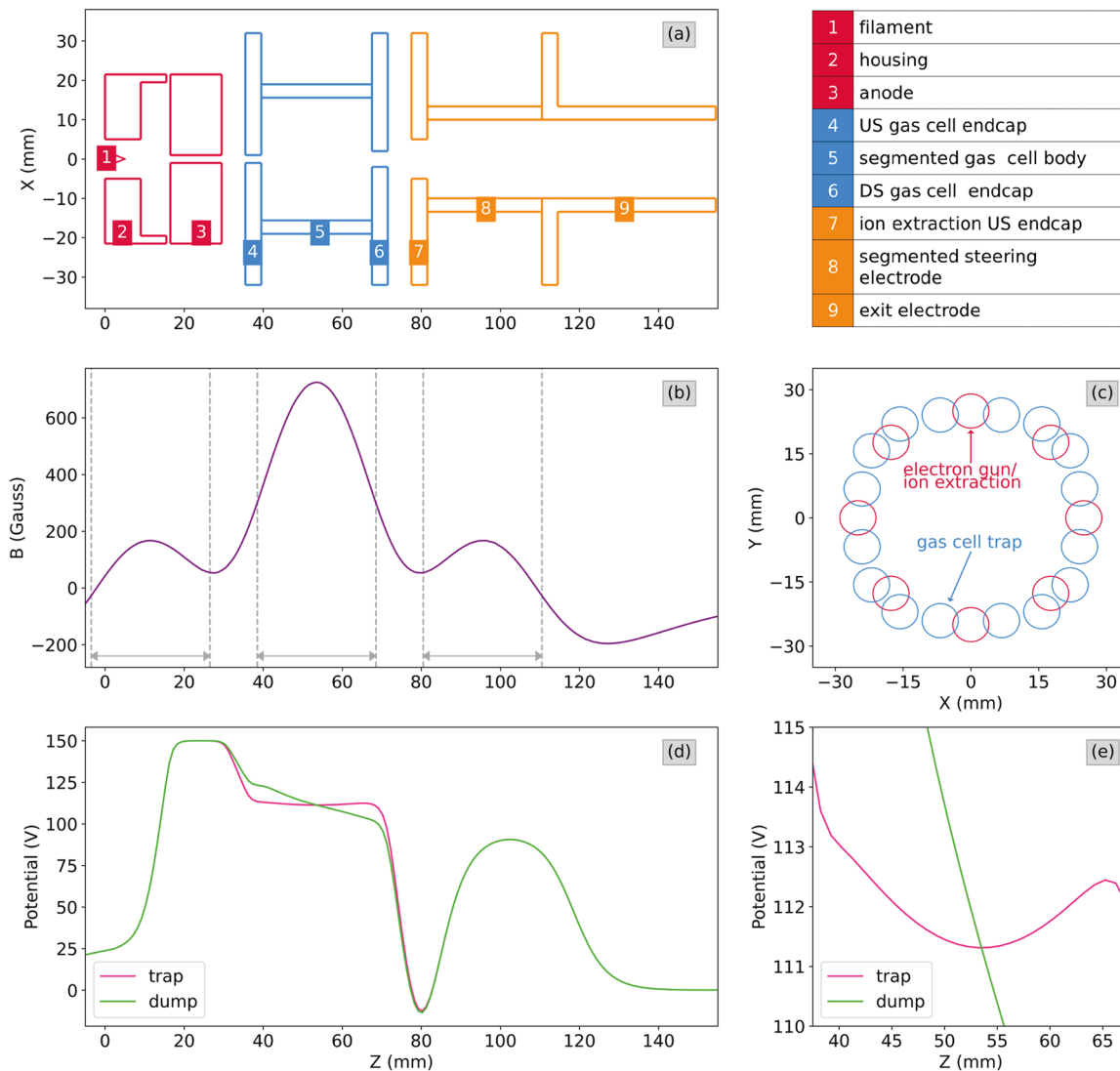
FIG. 1. (a) Schematic diagram of a cut view through the electrodes of the proton source; red: electron gun, blue: gas cell trap, and orange: ion extraction. (b) Z-component ($r = 0$) of the magnetic field strength (gauss) throughout the proton source; the dashed lines and arrows indicate the axial extent of the permanent magnets. (c) Azimuthal distribution of the magnets. They are evenly distributed ($r = 25$ mm) in rings of eight around the electron gun and ion extraction module (red). The gas cell trap is surrounded by two rings of eight with different radii ($r_1 = 25$ mm, $r_2 = 27$ mm) to allow space for the electrode contacts and gas input (blue). (d) Electrical potentials used during trapping (pink line) and extracting (green line) from the trap. (e) A closer view of the trapping/dumping potential.

surrounding housing electrode (~20 V). The anode (~100 V) extracts and focuses electrons out of the gun through a 2 mm aperture into the gas cell. Varying the filament heater current from 1.6 A/0.9 V to 2.1 A/1.58 V, electron emission currents between 2.1 pA and 4.8 μA were reproducibly generated. The emission current was determined by measuring the voltage drop over a resistor from the anode to ground. The resistors used in this measurement were chosen such that the anode potential did not change by more than ~0.5 V. The filament and housing were typically operated with a positive bias so that any grounded surface would repel the electrons.

B. Gas cell trap

This module serves three purposes. First, it contains the H_2 gas which the electron beam ionizes. Second, it produces magnetic and electric fields similar to those of a Penning trap to confine the ions before pulsed ejection. Finally, it allows the application of the RW to drive out contaminant ions.

The gas cell trap is constructed from six electrodes: an entrance cap, an end cap, and a body that is azimuthally segmented into four pieces, which can be individually biased. The entrance electrode has a 2 mm diameter, 4 mm long entrance tube. This allows the electron beam to enter and reduces the flow rate of H_2 into the

region between the cell and the gun. The exit electrode consists of a 5 mm long tube with a larger diameter of 4 mm. Although this allows more gas into the region between the cell and the ion extraction region, it also gives a larger solid angle for proton extraction. The central body is 28 mm long and is azimuthally split into four electrodes. The flow rate of hydrogen is externally controlled by a needle valve.

The gas cell can be operated without applying a trapping potential. In this mode, the ions produced by the electron beam are continuously accelerated out of the cell by a constant linear ramp-type potential [see Fig. 1(c) green line]. To produce a trap potential, the entrance and exit electrodes are biased higher than the central electrode [see Fig. 1(c) pink line]. The trap is emptied by pulsing the entrance (exit) electrode up (down), again forming a ramp-type potential, also allowing for time-of-flight spectroscopy.

Penning-type traps confine charged particles by superimposing a quadrupole electric field and a uniform magnetic field.[12] In the gas cell trap, the latter is provided by permanent magnets, which are a reasonable alternative when a fixed field value fulfills the requirements. In the present case, a total number of 32 neodymium (NdFeB) rod magnets (remanence B_r = 1.3 T, length = 30 mm, diameter = 8 mm) arranged as shown in Figs. 1(b) and 1(c) create a field with a strength of 73 mT in the center. The magnets around the electron gun and ion extraction module were added to prevent the axial magnetic field from changing direction between the modules. The Z-component at $r = 0$ of the magnetic field, simulated in COMSOL Multiphysics 5.5,[13] is shown in Fig. 1(b). The azimuthal asymmetry $\Delta B/B$ is ~4.13% at $r = 5$ mm off the trap axis. Producing such a field with normal conducting solenoid magnets as frequently used for Penning traps usually requires large magnets outside the vacuum vessel. The electrodes described above follow the design for geometrically compensated Penning traps.[14] They provide a suitable potential to trap protons at the simulated magnetic field strength.

The cross section for the process $e^- + H_2 \rightarrow 2e^- + H_2^+$ is an order of magnitude larger than for the dissociative ionization process $e^- + H_2 \rightarrow 2e^- + H + H^+$.[15] Many of the H_2^+ formed will also interact in the gas cell producing H_3^+ via the process $H_2^+ + H_2 \rightarrow H_3^+ + H$.[16] The dissociation of molecular hydrogen by electron impact has been well studied.[17,18] Dissociation proceeds either via the attractive $^2\Sigma_g^+$ state, which produces thermal to 3 eV protons,[17] or the repulsive $^2\Sigma_u^+$ state, which produces protons with energies up to 10 eV.[18] The source is designed such that in trapping mode, the RW will stabilize the motion of protons while removing the unwanted H_2^+ and H_3^+ ions. Ions heavier than H_3^+ do not fulfill the confinement condition $\left(\omega_c^2 > 2\omega_z^2\right.$, where ω_c is the cyclotron and ω_z is the axial frequency in the trap) of this Penning trap and leave the trap in less than 15 μs (for a well depth of ~1 V).

C. Extraction module

It is important to guide the protons into the Cusp trap on axis. This is carried out by the extraction module that focuses and steers the proton beam. Ions exiting the gas cell are accelerated by the ion extraction electrode, and can then be steered by a fourfold segmented cylinder. Electrostatic lenses can be produced between the steering electrode and the exit electrode for focusing the beam as it is accelerated out of the source.

III. CHARACTERIZATION

The proton source was installed into an ISO-160 cross with a turbo molecular pump providing the necessary pumping for the operation. It was characterized using a position-sensitive MCP delay-line detector (DLD40) from Roentdek,[19] installed in a second differentially pumped CF-100 cross downstream of the proton source. To protect the MCP from high-intensity ion beams, the filament was operated below nominal conditions. It was electrically heated by 1.725 A/1.07 V (I_0 ~ 84 pA) instead of 2.5–2.8 A.

The electron impact energy was varied by increasing or decreasing the gas cell potential with respect to the fixed potential of the electron gun filament. This also changes the energy of the ions extracted from the gas cell. For initial testing, the electron energy was set to 85 eV, near the peak of the proton production cross section.[15] This corresponds to an ion energy of 105 eV.

The source was first tested in continuous ion extraction mode, that is, without applying a trapping potential in the gas cell [see Fig. 1(d)]. Measurements were conducted to confirm the extraction module's ability to focus and move the ion beam before attempting to trap. Through variation of the extraction ring potential relative to the gas cell potential, the beam could either be focused or defocused at the detector, which was ~46 cm away from the source (measured to the center of the gas cell). The application of different voltages on the split electrode steered the beam in the desired direction.[20]

In trapping mode, the optimal well depth was determined first by maximizing the number of protons extracted from the source without the use of the RW. The different ion species were identified using time-of-flight spectroscopy (see below). Figure 2 shows the number of ions of each species measured for different well depths. The errors in this and all subsequent figures of count rates are counting statistics ($\sqrt{n}$). For this scan, the voltage on the entrance and exit electrodes was varied with all other potentials—and the overall energy—held constant. As the proton yield was the highest for a voltage difference of 3 V between the gas cell endcaps and the ring electrode, which corresponds to an on-axis well depth of 1.13 V, this well depth was selected for the operation of the source.
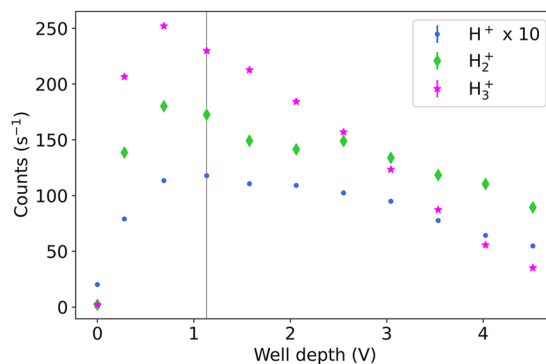

FIG. 2. Number of extracted protons (blue), H_2^+ (green), and H_3^+ (magenta) per second depending on the well depth (extraction frequency = 1.25 kHz, measurement time = 600 s, RW off). The line shows the selected well depth for the operation of the source.
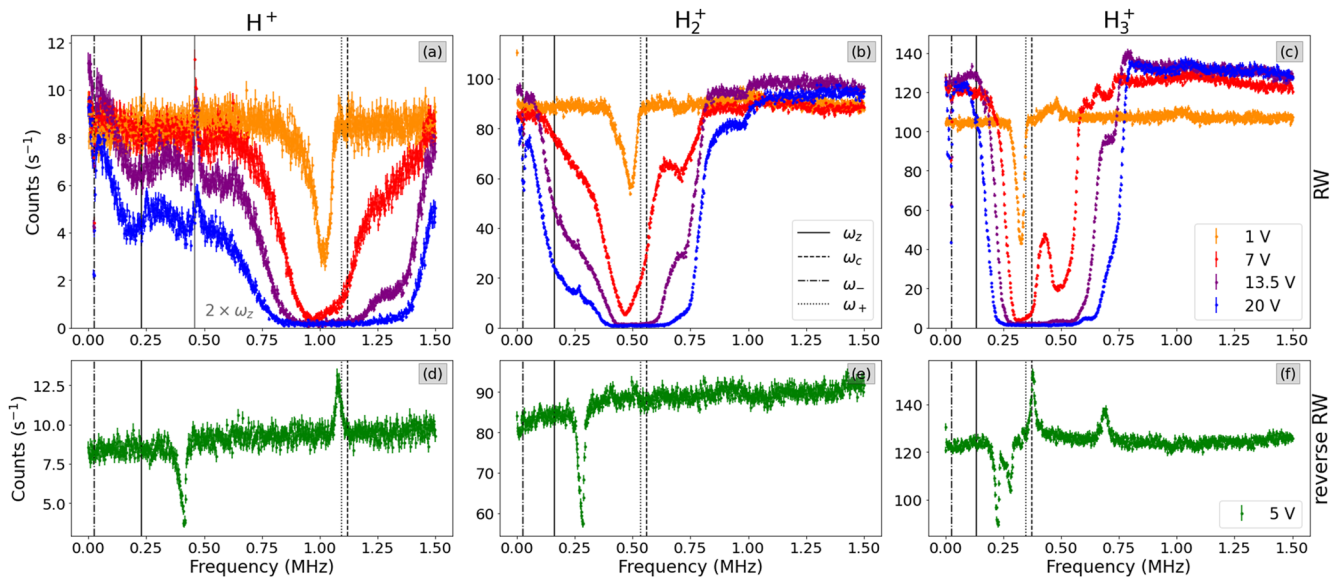
FIG. 3. Rotating wall frequency scans for (a) protons, (b) H_2^+, and (c) H_3^+. The figures compare the counts per second for 1 V (orange), 7 V (red), 13.5 V (purple), and 20 V (blue) RW amplitude. The scans at the bottom (d)–(f) are counter-rotating and performed at 5 V (green) RW amplitude. Also indicated on these figures in lines are the magnetron (dashed–dotted), axial bounce (solid), cyclotron (dashed), and modified cyclotron frequency (dotted).

Due to the significantly higher number of extracted H_2^+ and H_3^+ ions compared to protons, each exceeding the other by one order of magnitude, it was necessary to remove them from the system using the RW method. The frequency of the RW electric field was scanned, for different RW amplitudes, monitoring the rate of proton, H_2^+, and H_3^+ counts at the detector. Figures 3(a)–3(c) show the count rate obtained for each species as a function of RW frequency. Two Mini Circuits power splitters (ZSCJ-2-2+) were used to split the RW
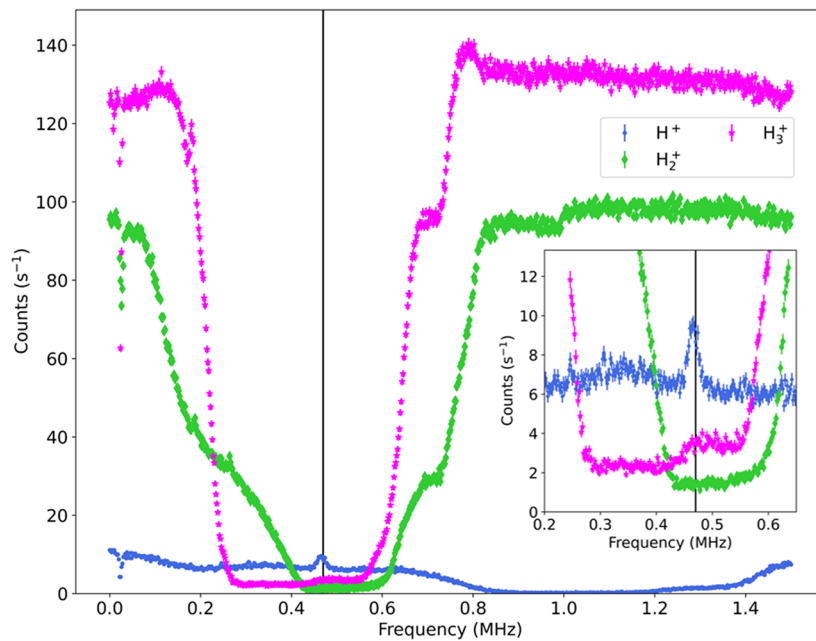

FIG. 4. Comparison of proton (blue), H_2^+ (green), and H_3^+ counts (magenta) for a fixed amplitude of 13.5 V [i.e., purple data of Figs. 3(a)–3(c)]. The solid black line shows the selected frequency of 0.47 MHz.

perturbations, reducing their amplitude in the process. The loss of the hereinafter-mentioned voltages can be found in the corresponding datasheet.[21] The RW was added to the bias voltage of the segmented ring electrode using an RF-coupling box.[20] The scans shown here were conducted at RW amplitudes of 1 V (orange points), 7 V (red points), 13.5 V (purple points), and 20 V (blue points). In all cases, it appears that the application of a frequency close to the magnetron frequency (ω_-), of a particular particle species, drove out each species (see also Fig. 4). In the case of protons, the application of a frequency close to twice the axial bounce frequency produced an increase in the observed count rate.

The main effect observable was the substantial loss of counts due to the dipolar excitation at the (mass-dependent) reduced cyclotron frequency. The effect broadened with the increase in RW amplitude. This cleaning of ion species via deliberate radial ejection has been used in different Penning trap setups such as ISOLTRAP[22] and JYFLTRAP.[23]

Consider Fig. 4, which compares the count rates for protons, H_2^+, and H_3^+ for the 13.5 V scan: by selecting a frequency close to twice the axial bounce frequency for protons (0.47 MHz), the H^+ count rate was preserved, whereas, in the case of H_2^+ and H_3^+, the rates were greatly reduced by an apparent coupling to the reduced cyclotron motion. For a counter-rotating field [Figs. 3(d)–3(f)], an increase in protons and H_3^+ close to their cyclotron frequency was observed, whereas no such effect could be seen for H_2^+ ions. Furthermore, the counter-rotating field removed every species at roughly twice the (species-dependent) axial bounce frequency. However, this rotating field direction was not chosen for further operation, as the co-rotating field both preserves the proton yield and simultaneously drives out H_2^+ and H_3^+.

The RW amplitude was optimized by scanning the oscillating voltage V_{pp} applied to the electrodes at the fixed proton peak frequency of 0.47 MHz. As may be expected, Figs. 3(a) and 5 show that the proton count rate was reasonably constant across the investigated range. The number of H^+ exceeds H_2^+ and H_3^+ counts for $V_{pp} \geq 10$.

The largest difference between the proton and other ion count rates was achieved at about 13.5 V. At this point, (8.67 ± 0.38) s^{-1}
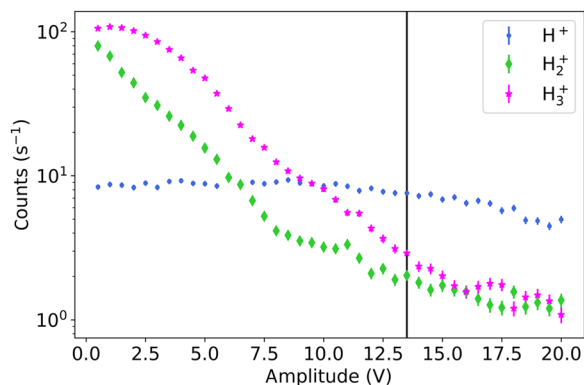
protons, (1.38 ± 0.15) s^{-1} H_2^+, and (3.45 ± 0.24) s^{-1} H_3^+ were measured.

A time-of-flight spectrum at these optimum values is shown in Fig. 6 (orange). The proton peak is well-defined at 4.1 μs. The H_2^+ and H_3^+ peaks at 5.8 and 7.1 μs, respectively, are visible but smaller than the proton peak. This figure also shows the time-of-flight spectrum without the application of the RW, in red.

The extraction of 10 000 ions of each species was simulated in SIMION 8.1, and the time-of-flight to the detector was recorded. These results are included in Fig. 6 for comparison. In reality, due to the cross sections,[15] we expect ~10 times less H^+ than H_2^+ in the trap. At the voltage chosen for the MCP operation, the detection efficiencies for all species are the same.[24] The simulations showed a total arrival efficiency at the detector (combination of the ion extraction efficiency from the source and the transport efficiency to the detector) of $\approx$11.6% for protons, $\approx$4.3% for H_2^+, and $\approx$3.2% for H_3^+. While the extraction efficiency did not depend greatly on the axial position of the particles in the gas cell, on-axis particles were favored with the extraction efficiency dropping to half of its maximum at $r = 2$ mm. Any further interactions between the ions and H_2 or residual gas on the way to the detector were not taken into account. The lifetime of the protons in the trap was estimated by measuring the number of protons produced for different trapping times. The trapping time was varied by changing the extraction frequency while keeping the extraction pulse width constant, that is, the trap was filled for different time spans. An exponential saturation curve of the form $N \sim a \cdot \exp[-t/\tau] + b$ was fitted, where τ is the proton lifetime in the trap.[20] Figure 7(a) shows that the lifetime decreased with increasing gas pressure, indicating that a higher collision rate was detrimental to stable trapping. The lifetime also depended on the RW amplitude, peaking around 10–15 V. The stabilization of protons in the trap due to the application of twice the axial bounce frequency improves with increasing amplitudes, however, and so does the power broadening of the radial ejection at the reduced cyclotron frequency. The reduction in lifetime at higher amplitudes could therefore be attributed to the second effect becoming dominant.

FIG. 5. Amplitude scan for protons (blue), H_2^+ (green), and H_3^+ (magenta) at a RW frequency of 0.47 MHz. The solid black line shows the selected amplitude of 13.5 V.
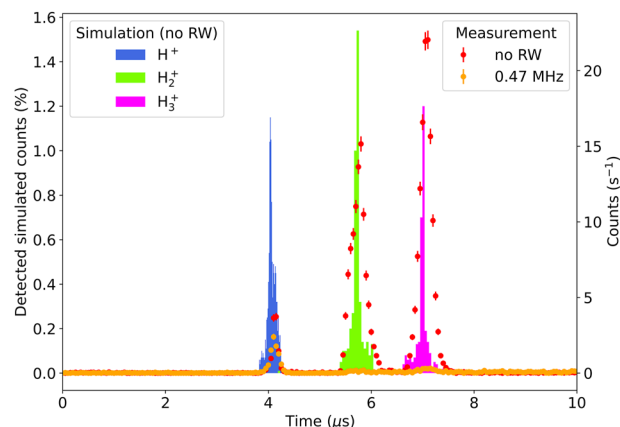

FIG. 6. Measured time-of-flight spectrum with (orange) and without (red) RW ($f = 0.47$ MHz, $V_{pp} = 13.5$ V), and simulation of the extraction out of the gas cell for protons (blue), H_2^+ (green), and H_3^+ (magenta).
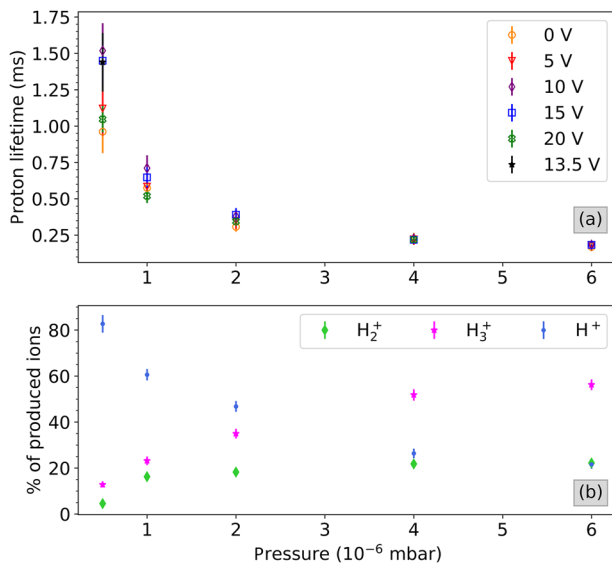
FIG. 7. (a) Lifetime of protons in the gas cell trap as a function of vacuum chamber pressure and RW amplitude at a RW frequency of 0.47 MHz; (b) Percentages of extracted protons (blue), H_2^+ (green), and H_3^+ (magenta) for different vacuum chamber pressures at RW settings (f = 0.47 MHz, V_{pp} = 13.5 V).

Figure 7(b) shows the fraction of the extracted ions species for different pressures, using the optimal RW settings (f = 0.47 MHz, V_{pp} = 13.5 V). The unfavorable reduction in the H^+-ratio at higher pressures might be attributed to the larger number of secondary interactions undergone by protons in the extraction module.

The pressure reported in Fig. 7 was measured in the proton source vacuum chamber and does not correspond to the pressure in the gas cell. A pressure simulation of the whole system was therefore conducted in Molflow+[25] using 3D renderings of the source and a to-scale representation of the vacuum system. Pumping speeds were set according to the values given by pump manufacturers and the H_2 flow rate was varied. We obtain that the pressures in the gas cell are ~120 times larger than the pressure measured at the pressure gauge. For the electron gun and ion extraction module, they are both higher by about a factor of 2.

Most of the work described here was conducted at 1×10^{-6} mbar. This would correspond to a gas cell pressure of ~ 1.2×10^{-4} mbar.

IV. SUMMARY

A simple low energy proton source, based on electron impact ionization of H_2 in a Penning trap gas cell, was constructed and characterized. It will be used by the ASACUSA Cusp experiment for comparative matter experiments, especially when antiprotons are unavailable. As expected, in agreement with the H_2 ionization cross section, the number of protons produced is approximately one order of magnitude lower than the H_2^+ and H_3^+ ions. A rotating wall electric field was applied to the gas cell to preserve the number of protons and reduce the number of H_2^+ and H_3^+ ions. This technique was successfully applied to reduce the number of background ions by an order of magnitude while maintaining the number of protons.

Energy tunable pulses of ~9 protons/second (extraction frequency = 500 Hz, vacuum chamber pressure = 0.5×10^{-6} mbar) were produced for the low electron intensity of ~84 pA. These pulses have minimal contamination of ~5.5% H_2^+ and ~15.5% H_3^+. Although our single-particle detector does not allow for high-intensity rate measurements, our results would extrapolate to ~10^5 protons/s when the electron emission is raised to ~4.8 μA. The proton source has now been paired with a pumping restriction (inner diameter = 6 mm, length = 10 cm) and installed into the ASACUSA apparatus. It fulfills the vacuum requirement (pressure = 1×10^{-8} mbar downstream of pumping restriction) for its operation within the ASACUSA experiment and allows proton plasma experiments whenever antiprotons are not available. Furthermore, it may also be used to test new equipment integrated into the $\overline{p}$-beamline.

AUTHOR DECLARATIONS

Conflict of Interest

The authors have no conflicts to disclose.

Author Contributions

A. Weiser: Formal analysis (lead); Investigation (lead); Visualization (lead); Writing - Original draft (lead); Software (equal); Validation (equal). **A. Lanz:** Writing - reviewing & editing (equal); Investigation (equal); Software (equal); Validation (equal). **E. D. Hunter:** Methodology (equal); Validation (equal); Writing - reviewing & editing (equal). **M. C. Simon:** Conceptualization (lead); Funding acquisition (equal); Resources (equal); Writing – reviewing & editing (equal); Supervision (supporting). **E. Widmann:** Funding acquisition (supporting); Supervision (supporting); Writing - reviewing & editing (supporting). **D. J. Murtagh:** Conceptualization (equal); Funding acquisition (lead); Methodology (equal); Project administration (lead); Software (supporting); Supervision (lead); Validation (equal); Visualization (supporting); Writing - reviewing & editing (equal).

DATA AVAILABILITY

The data that support the findings of this study are available from the corresponding author upon reasonable request.

REFERENCES

[1] A. Mohri and Y. Yamazaki, "A possible new scheme to synthesize antihydrogen and to prepare a polarised antihydrogen beam," Europhys. Lett. **63**, 207 (2003).
[2] E. Widmann, R. S. Hayano, M. Hori, and T. Yamazaki, "Measurement of the hyperfine structure of antihydrogen," Nucl. Instrum. Methods Phys. Res., Sect. B **214**, 31 (2004).

03 November 2023 18:52:04

[3]B. Kolbinger, C. Amsler, S. Cuendis, H. Breuker, A. Capon, G. Costantini, P. Dupré, M. Fleck, A. Gligorova, H. Higaki, Y. Kanai, V. Kletzl, N. Kuroda, A. Lanz, M. Leali, V. Mäckel, C. Malbrunot, V. Mascagna, O. Massiczek, Y. Matsuda, D. J. Murtagh, Y. Nagata, A. Nanda, L. Nowak, B. Radics, C. Sauerzopf, M. Simon, M. Tajima, H. Torii, U. Uggerhøj, S. Ulmer, L. Venturelli, A. Weiser, M. Wiesinger, E. Widmann, T. Wolz, Y. Yamazaki, and J. Zmeskal, "Measurement of the principal quantum number distribution in a beam of antihydrogen atoms," Eur. Phys. J. D **75**, 91 (2021).

[4]N. Kuroda, S. Ulmer, D. J. Murtagh, S. Van Gorp, Y. Nagata, M. Diermaier, S. Federmann, M. Leali, C. Malbrunot, V. Mascagna, O. Massiczek, K. Michishio, T. Mizutani, A. Mohri, H. Nagahama, M. Ohtsuka, B. Radics, S. Sakurai, C. Sauerzopf, K. Suzuki, M. Tajima, H. A. Torii, L. Venturelli, B. Wünschek, J. Zmeskal, N. Zurlo, H. Higaki, Y. Kanai, E. Lodi Rizzini, Y. Nagashima, Y. Matsuda, E. Widmann, and Y. Yamazaki, "A source of antihydrogen for in-flight hyperfine spectroscopy," Nat. Commun. **5**, 3089 (2014).

[5]W. Quint, R. Kaiser, D. Hall, and G. Gabrielse, "(Anti)hydrogen recombination studies in a nested Penning trap," Hyperfine Interact. **76**, 181 (1993).

[6]P. Roychowdhury, H. Kewlani, L. Mishra, S. Gharat, and R. K. Rajawat, "Emittance and proton fraction measurement in high current electron cyclotron resonance proton ion source," Nucl. Instrum. Methods Phys. Res., Sect. A **795**, 45 (2015).

[7]C. Baumgarten, A. Barchetti, H. Einenkel, D. Goetz, and P. A. Schmelzbach, "A compact electron cyclotron resonance proton source for the Paul Scherrer Institute's proton accelerator facility," Rev. Sci. Instrum. **82**, 053304 (2011).

[8]J. Bin, K. Allinger, W. Assmann, G. Dollinger, G. A. Drexler, A. A. Friedl, D. Habs, P. Hilz, R. Hoerlein, N. Humble, S. Karsch, K. Khrennikov, D. Kiefer, F. Krausz, W. Ma, D. Michalski, M. Molls, S. Raith, S. Reinhardt, B. Röper, T. E. Schmid, T. Tajima, J. Wenz, O. Zlobinskaya, J. Schreiber, and J. J. Wilkens, "A laser-driven nanosecond proton source for radiobiological studies," Appl. Phys. Lett. **101**, 243701 (2012).

[9]M. Barberio, M. Sciscò, S. Vallières, F. Cardelli, S. N. Chen, G. Famulari, T. Gangolf, G. Revet, A. Schiavi, M. Senzacqua, and P. Antici, "Laser-accelerated particle beams for stress testing of materials," Nat. Commun. **9**, 372 (2018).

[10]T. Murböck, S. Schmidt, Z. Andelkovic, G. Birkl, W. Nörtershäuser, and M. Vogel, "A compact source for bunches of singly charged atomic ions," Rev. Sci. Instrum. **87**, 043302 (2016).

[11]E. M. Hollmann, F. Anderegg, and C. F. Driscoll, "Confinement and manipulation of non-neutral plasmas using rotating wall electric fields," Phys. Plasmas **7**, 2776 (2000).

[12]K. Blaum, Y. N. Novikov, and G. Werth, "Penning traps as a versatile tool for precise experiments in fundamental physics," Contemp. Phys. **51**, 149 (2010).

[13]COMSOL AB, Comsol Multiphysics® v. 5.5, Stockholm, Sweden (2020).

[14]G. Gabrielse and F. Mackintosh, "Cylindrical penning traps with orthogonalized anharmonicity compensation," Int. J. Mass Spectrom. Ion Processes **57**, 1 (1984).

[15]H. C. Straub, P. Renault, B. G. Lindsay, K. A. Smith, and R. F. Stebbings, "Absolute partial cross sections for electron-impact ionization of H_2, N_2, and O_2 from threshold to 1000 eV," Phys. Rev. A: At., Mol., Opt. Phys. **54**, 2146 (1996).

[16]A. V. Phelps, "Cross sections and swarm coefficients for H^+, H_2^+, H_3^+, H, H_2, and H^- in H_2 for energies from 0.1 eV to 10 keV," J. Phys. Chem. Ref. Data **19**, 653 (1990).

[17]G. H. Dunn and L. J. Kieffer, "Dissociative ionization of H_2: A study of angular distributions and energy distributions of resultant fast protons," Phys. Rev. **132**, 2109 (1963).

[18]A. Crowe and J. W. McConkey, "Dissociative ionization by electron impact. I. Protons from H_2," J. Phys. B: At. Mol. Phys. **6**, 2088 (1973).

[19]O. Jagutzki, J. Lapington, L. Worth, U. Spillman, V. Mergel, and H. Schmidt-Böcking, "Position sensitive anodes for MCP read-out using induced charge measurement," Nucl. Instrum. Methods Phys. Res., Sect. A **477**, 256 (2002).

[20]A. Weiser, "A low energy proton source for ASACUSA's matter studies," Master's thesis, University of Vienna, 2020.

[21]Mini Circuits®, Coaxial Power Splitter/Combiner ZSCJ-2-2+, url: https://www.minicircuits.com/pdfs/ZSCJ-2-2+.pdf

[22]K. Blaum, D. Beck, G. Bollen, P. Delahaye, C. Guénaut, F. Herfurth, A. Kellerbauer, H.-J. Kluge, D. Lunney, S. Schwarz, L. Schweikhard, and C. Yazidjian, "Population inversion of nuclear states by a penning trap mass spectrometer," Europhys. Lett. **67**, 586 (2004).

[23]V. Kolhinen, S. Kopecky, T. Eronen, U. Hager, J. Hakala, J. Huikari, A. Jokinen, A. Nieminen, S. Rinta-Antila, J. Szerypo, and J. Äystö, "JYFLTRAP: a cylindrical Penning trap for isobaric beam purification at IGISOL," Nucl. Instrum. Phys. Res., Sect. A **528**, 776 (2004).

[24]B. Peko and T. Stephen, "Absolute detection efficiencies of low energy H, H^-, H^+, H_2^+ and H_3^+ incident on a multichannel plate detector," Nucl. Instrum. Methods Phys. Res., Sect. B **171**, 597 (2000).

[25]R. Kersevan and M. Ady, Recent developments of Monte-Carlo codes Molflow+ and Synrad+, in *Proceedings of the 10th International Particle Accelerator Conference* (JACoW, 2019), pp. 1327–1330.

03 November 2023 18:52:04